Int. J. Electron. Commun. (AEÜ) 84 (2018) 8–12

Contents lists available at ScienceDirect

Int. J. Electron. Commun. (AEÜ)

journal homepage: www.elsevier.com/locate/aeue

Regular paper

Covariance matrix based fast smoothed sparse DOA estimation with partly calibrated array

Jing Liu[a,b], Weidong Zhou[a,*], Defeng (David) Huang[b], Filbert H. Juwono[c]

[a] College of Automation, Harbin Engineering University, Harbin 150001, China
[b] School of Electrical, Electronic and Computer Engineering, The University of Western Australia, Perth, WA 6009, Australia
[c] Department of Electrical Engineering, Universitas Indonesia, Depok, West Java 16424, Indonesia

ARTICLE INFO

Keywords:
Direction-of-arrival estimation
Fast signal reconstruction
Partly calibrated array

ABSTRACT

To solve the problem of direction-of-arrival (DOA) estimation for partly calibrated array, a new gain-phase error matrix estimation scheme and a smoothed sparse signal reconstruction method tailored for the complex-valued covariance matrix are proposed. In the proposed method, DOA estimation is achieved by employing the structure of the covariance matrix for the error matrix estimation and the complex-valued gradient matrix based fast non-convexity data reconstruction. The proposed method has much faster computational speed than other sparse DOA estimation methods with partly calibrated array. In addition, simulation results show that it performs well and is independent of the errors.

1. Introduction

Direction-of-arrival (DOA) estimation plays an important role in practical applications, such as radar and sonar. Traditional super-resolution DOA estimation algorithms [1–5], e.g. MUSIC [1] and ESPRIT [2], are subspace based. The emerging sparse representation (SR) based DOA estimation has attracted increasing attention due to its better adaptation to snapshot deficiency and superior performance in low signal-to-noise ratio (SNR). Regarding the methods for the sparse signal reconstruction [6–15], the widely employed l_1-norm algorithms including l_1-SVD [6], have demonstrated excellent performance with reasonable computational complexity. By contrast, the complexity of the sparse Bayesian learning (SBL) methods [9] is much higher. Compared with the l_1-norm minimization, it has been shown in [13] that the smoothed l_0-norm [11–13] can provide similar or better signal recovery with significantly reduced computational resources required. Recently, by reconstructing a signal power vector, we have proposed a re-weighted smoothed l_0-norm algorithm [14] for DOA estimation. The high-order cumulants based joint smoothed l_0-norm method [15] has been proposed to deal with the colored and white Gaussian noises. However, it requires non-Gaussian signals and a large number of snapshots to estimate the cumulants accurately.

Most subspace and SR based methods assume that the array model is ideal with precisely known steering vector [1–15]. However, in practice, the unknown gain-phase errors seriously degrade the performance of these methods. To cope with partly calibrated array, some calibrated methods [16–19] have been proposed based on the different properties of the signal and noise subspaces. The Hadamard product methods [16,17] and the eigenstructure method [18] all involve two-dimensional spatial spectrum searches, which lead to high computational complexity. The ESPRIT-like algorithm [19] avoids the spectrum search, with the cost of the loss of array aperture. Concerning the sparse representation based DOA estimation with partly calibrated array, the adaptive SR algorithm [20] dynamically adjusts the overcomplete basis with an initial unit error matrix. The joint optimization method [21] for the DOA estimation and the array error matrix estimation solves a non-convex optimization problem with two convex optimization sub-problems. Both methods in [20,21] perform the l_1-norm minimization based iterations, by randomly initializing the unknown gain-phase error matrix as an unit matrix or random matrix. Therefore, they require enormous computation time, and their convergence cannot be guaranteed, leading to large estimation errors.

In this paper, we propose a new gain-phase error estimation scheme, and a complex-valued covariance matrix based fast smoothed sparse DOA estimation algorithm for partly calibrated array. The complexity of the proposed method is much lower than the sparse algorithms in [20,21]. Making full use of the covariance matrix structure of the received signals, the proposed method first estimates the gain-phase error matrix. Then it designs a continuous function, which is tailored for the complex-valued covariance matrix based sparse representation framework containing the estimated error matrix. Finally, inspired by [11–14], a complex-valued gradient matrix based fast smoothed sparse

* Corresponding author.
E-mail addresses: liujing@hrbeu.edu.cn (J. Liu), zhouweidong@hrbeu.edu.cn (W. Zhou), david.huang@uwa.edu.au (D.D. Huang), filbert@ieee.org (F.H. Juwono).

https://doi.org/10.1016/j.aeue.2017.10.026
Received 13 September 2017; Accepted 18 October 2017

signal reconstruction is employed to handle the DOA estimation problem for partly calibrated array. Simulation results show that the proposed error matrix estimation can also be applied in other methods to eliminate the effect of the gain-phase errors. With lower computational complexity, the new algorithm has much faster speed than the existing sparse DOA estimation methods with partly calibrated array, including [20,21].

2. Problem formulation

Consider a partly calibrated uniform linear array (ULA) with N half-wavelength interspaced sensors. There are $P < N$ narrowband far-field signals located at $\{\theta_1,\theta_2,\ldots,\theta_P\}$. Without loss of generality, the first $m > 1$ sensors are assumed to be well calibrated. The gain-phase errors of the last $N-m$ sensors are unknown. The received data vector is [16–19]

$$\mathbf{x}(t_i) = \mathbf{\Gamma}\mathbf{A}\mathbf{s}(t_i) + \mathbf{n}(t_i), \quad i = 1,2,\ldots,T \tag{1}$$

where $\mathbf{\Gamma} = \mathrm{diag}[\gamma_1 e^{j\varphi_1},\gamma_2 e^{j\varphi_2},\ldots,\gamma_N e^{j\varphi_N}]$ is the diagonal gain-phase error matrix with $\{\gamma_n\}_{n=1}^m = \{e^{j\varphi_n}\}_{n=1}^m = 1$. T is the number of snapshots. The steering matrix $\mathbf{A} = [\mathbf{a}(\theta_1),\ldots,\mathbf{a}(\theta_P)]$ is composed of $\mathbf{a}(\theta_p) = \left[1,e^{j\pi\sin(\theta_p)},e^{j\pi 2\sin(\theta_p)},\ldots,e^{j\pi(N-1)\sin(\theta_p)}\right]^{\mathrm{T}}$. $\mathbf{s}(t_i)$ and $\mathbf{n}(t_i)$ are the signal and noise vectors, respectively. The signals and noises are both zero-mean Gaussian with the power $\{\rho_p\}_{p=1}^P$ and $\bar{\tau}$, respectively. The signals for different targets contain different reflection coefficients [14,22]. They are mutually uncorrelated, and independent of the noises. The covariance matrix of the white Gaussian noises is commonly assumed to be $\mathbf{R}_n = \bar{\tau}\mathbf{I}_N$, and $\mathbf{I}_N$ denotes an $N \times N$ unit matrix. From Eq. (1), the covariance matrix of the received signal is as follows

$$\mathbf{R}_x = \mathbf{\Gamma}\mathbf{A}\mathbf{R}_s(\mathbf{\Gamma}\mathbf{A})^H + \mathbf{R}_n = \mathbf{\Gamma}\mathbf{A}\mathbf{R}_s(\mathbf{\Gamma}\mathbf{A})^H + \bar{\tau}\mathbf{I}_N \tag{2}$$

where $\mathbf{R}_s = \mathrm{diag}[\rho_1,\ldots,\rho_P]$, and $(\cdot)^H$ denotes the conjugate-transpose. Consequently, if the estimates of $\mathbf{R}_x$ and $\bar{\tau}$ are available, we have

$$\widetilde{\mathbf{R}}_{\tilde{x}} = \mathbf{R}_x - \bar{\tau}\mathbf{I}_N = \mathbf{\Gamma}\mathbf{A}\mathbf{R}_s(\mathbf{\Gamma}\mathbf{A})^H \tag{3}$$

where $\widetilde{\mathbf{R}}_{\tilde{x}}$ is the covariance matrix corresponding to $\mathbf{\Gamma}\mathbf{A}\mathbf{s}(t_i)$.

3. Proposed method

3.1. Covariance matrix based gain-phase error estimation

In the following, according to the structure of $\widetilde{\mathbf{R}}_{\tilde{x}}$, useful covariances are extracted to estimate the gain-phase error matrix. The $(i+1,i)$th element of $\widetilde{\mathbf{R}}_{\tilde{x}}$ is represented as follows

$$\left(\widetilde{\mathbf{R}}_{\tilde{x}}\right)_{(i+1,i)} = (\mathbf{\Gamma}\mathbf{A})_{(i+1,:)}\mathbf{R}_s[(\mathbf{\Gamma}\mathbf{A})_{(i,:)}]^H \tag{4}$$

where $(\cdot)_{(q,:)}$ denotes the qth row in a matrix. The detailed expression of $(\widetilde{\mathbf{R}}_{\tilde{x}})_{(i+1,i)}$ is as follows

$$\left(\widetilde{\mathbf{R}}_{\tilde{x}}\right)_{(i+1,i)} = \sum_{p=1}^{P} \gamma_i\gamma_{i+1}e^{j\varphi_{i+1}-j\varphi_i}e^{j\pi\sin(\theta_p)}\rho_p \tag{5}$$

for $i = 1,2,\ldots,N-1$. Let

$$Q_1 = \sum_{p=1}^{P} e^{j\pi\sin(\theta_p)}\rho_p \tag{6}$$

Then based on Eq. (5), a vector containing all of the i indices can be constructed as

$$\begin{aligned}\vec{\mathbf{v}}_1 &= [(\widetilde{\mathbf{R}}_{\tilde{x}})_{(2,1)},(\widetilde{\mathbf{R}}_{\tilde{x}})_{(3,2)},\ldots,(\widetilde{\mathbf{R}}_{\tilde{x}})_{(N,N-1)}]^T\\ &= Q_1\left[\gamma_1\gamma_2 e^{j(\varphi_2-j\varphi_1)},\ldots,\gamma_{N-1}\gamma_N e^{j(\varphi_N-\varphi_{N-1})}\right]^T\end{aligned} \tag{7}$$

where $(\cdot)^T$ denotes the transpose. From Eq. (7), we can construct the following continuous multiplication operator

$$\begin{aligned}\prod_{i=1}^{k_1}\vec{\mathbf{v}}_1(i) &= Q_1^{k_1}\gamma_1\gamma_2\gamma_2\gamma_3\cdots\gamma_{k_1}\gamma_{k_1+1}e^{j[\sum_{i=1}^{k_1}(\varphi_{i+1}-j\varphi_i)]}\\ &= Q_1^{k_1}\gamma_{k_1+1}e^{j\varphi_{k_1+1}}\prod_{i=1}^{k_1}\gamma_i^2\end{aligned} \tag{8}$$

with $\gamma_1 = 1$, and $k_1 = m,m+1,\ldots,N-1$. In Eq. (8), $\vec{\mathbf{v}}_1(i)$ is the ith element of $\vec{\mathbf{v}}_1$. To estimate the gain-phase errors, the estimation of the continuous multiplication of γ_i is required. Note that there is no need to obtain each gain error γ_i separately. $(\widetilde{\mathbf{R}}_{\tilde{x}})_{(i,i)}$ is given by

$$\begin{aligned}(\widetilde{\mathbf{R}}_{\tilde{x}})_{(i,i)} &= (\mathbf{\Gamma}\mathbf{A})_{(i,:)}\mathbf{R}_s[(\mathbf{\Gamma}\mathbf{A})_{(i,:)}]^H\\ &= \sum_{p=1}^{P}\gamma_i^2\rho_p\end{aligned} \tag{9}$$

Then we can construct another vector as follows

$$\begin{aligned}\vec{\mathbf{v}}_2 &= [(\widetilde{\mathbf{R}}_{\tilde{x}})_{(1,1)},(\widetilde{\mathbf{R}}_{\tilde{x}})_{(2,2)},\ldots,(\widetilde{\mathbf{R}}_{\tilde{x}})_{(N,N)}]^T\\ &= \sum_{p=1}^{P}\rho_p[\gamma_1^2,\gamma_2^2,\ldots,\gamma_N^2]^T\end{aligned} \tag{10}$$

Therefore, we have

$$\prod_{i=1}^{k_2}\vec{\mathbf{v}}_2(i) = \left(\sum_{p=1}^{P}\rho_p\right)^{k_2}\prod_{i=1}^{k_2}\gamma_i^2 \tag{11}$$

where the range of k_2 can be from $k_2 = 1$ to $k_2 = N$. Let the value of k_2 in Eq. (11) be the same as the value of k_1 in Eq. (8), i.e. $k_2 = k_1 = k$, it can be derived that

$$\begin{aligned}\prod_{i=1}^{k}\vec{\mathbf{v}}_1(i)\Big/\prod_{i=1}^{k}\vec{\mathbf{v}}_2(i) &= \gamma_{k+1}e^{j\varphi_{k+1}}\left[\frac{Q_1}{\sum_{p=1}^{P}\rho_p}\right]^k\\ &= \gamma_{k+1}e^{j\varphi_{k+1}}(Q_1/Q_2)^k\end{aligned} \tag{12}$$

where $k = m,m+1,\ldots,N-1$, and $Q_2 = \sum_{p=1}^{P}\rho_p$. Note that with regard to Q_1 and Q_2 in Eq. (12), according to Eqs. (7) and (10), the first $m-1$ elements in $\vec{\mathbf{v}}_1$ and the first m elements in $\vec{\mathbf{v}}_2$ satisfy

$$\begin{aligned}&\vec{\mathbf{v}}_1(1) = \vec{\mathbf{v}}_1(2) = \cdots = \vec{\mathbf{v}}_1(m-1) = Q_1\\ &\vec{\mathbf{v}}_2(1) = \vec{\mathbf{v}}_2(2) = \cdots = \vec{\mathbf{v}}_2(m) = Q_2\end{aligned} \tag{13}$$

From Eq. (12), the proposed gain-phase error matrix estimation in the proposed method is formulated as

$$\mathbf{\Gamma}_{(k+1,k+1)} = \frac{\prod_{i=1}^{k}\vec{\mathbf{v}}_1(i)/\prod_{i=1}^{k}\vec{\mathbf{v}}_2(i)}{(Q_1/Q_2)^k} \tag{14}$$

for $k = m,m+1,\ldots,N-1$. In practice, $\mathbf{R}_x$ is estimated from $\hat{\mathbf{R}}_x = \frac{1}{T}\sum_{i=1}^{T}\mathbf{x}(t_i)\mathbf{x}^H(t_i)$. Furthermore, $\bar{\tau}$ is calculated by $\hat{\bar{\tau}} = \frac{1}{N-P}\sum_{i=P+1}^{N}\tau_i$ with τ_i being the ith eigenvalue of $\hat{\mathbf{R}}_x$ in descending order. Then in Eq. (14), the estimation of $\vec{\mathbf{v}}_1$ and $\vec{\mathbf{v}}_2$, denoted by $\hat{\vec{\mathbf{v}}}_1$ and $\hat{\vec{\mathbf{v}}}_2$, is extracted from $\hat{\widetilde{\mathbf{R}}}_{\tilde{x}} = \hat{\mathbf{R}}_x - \hat{\bar{\tau}}\mathbf{I}_N$. Based on Eq. (13), making the best of the information corresponding to the well-calibrated sensors, Q_1 and Q_2 in Eq. (14) can be approximated by

$$\begin{aligned}Q_1 &\approx \frac{1}{m-1}\sum_{i=1}^{m-1}\hat{\vec{\mathbf{v}}}_1(i)\\ Q_2 &\approx \frac{1}{m}\sum_{i=1}^{m}\hat{\vec{\mathbf{v}}}_2(i)\end{aligned} \tag{15}$$

With the error matrix $\mathbf{\Gamma}$ obtained from Eq. (14), DOA estimation can then be achieved by employing conventional approaches, such as the subspace based MUSIC [1] and the l_1-norm based l_1-SVD [6]. However, the subspace methods rely heavily on the precision of the steering matrix, and their performance is poor for snapshot deficiency and low SNR. Although the sparse signal recovery algorithms can overcome these shortcomings, the widely used l_1-norm methods are time consuming. Therefore, in the following, with the estimated error matrix $\boldsymbol{\Gamma}$, we further design a fast sparse signal reconstruction scheme tailored for the complex-valued covariance matrix, to solve those problems existing in the DOA estimation methods for partly calibrated array.

3.2. Covariance matrix based fast sparse DOA estimation

As the on-grid SR-based DOA estimation [14], a discrete sample grid $\{\hat{\theta}_l\}_{l=1}^{L}$ containing all directions of interest is required. Let $\hat{\mathbf{A}}_{\hat{\theta}} = [\mathbf{a}(\hat{\theta}_1),\mathbf{a}(\hat{\theta}_2),\ldots,\mathbf{a}(\hat{\theta}_L)]$ be a complete dictionary. Signal recovery is regarded as measuring the sparsity of a complex-valued matrix $\hat{\mathbf{S}}_{\hat{\theta}}$, which subjects to $\widetilde{\mathbf{R}}_{\widetilde{x}} = \boldsymbol{\Gamma}\hat{\mathbf{A}}_{\hat{\theta}}\hat{\mathbf{S}}_{\hat{\theta}}$. Thus, we define a vector $\widetilde{\mathbf{s}}_{\hat{\theta}}$ whose ith element is the l_2-norm of the ith row in $\hat{\mathbf{S}}_{\hat{\theta}}$. The signal recovery for DOA estimation can be formulated as

$$\hat{\mathbf{S}}_{\hat{\theta}} = \arg\min(\|\widetilde{\mathbf{s}}_{\hat{\theta}}\|_0), \quad \text{s.t.} \quad \widetilde{\mathbf{R}}_{\widetilde{x}} = \boldsymbol{\Gamma}\hat{\mathbf{A}}_{\hat{\theta}}\hat{\mathbf{S}}_{\hat{\theta}} \tag{16}$$

where $\hat{\mathbf{S}}_{\hat{\theta}}$ has the same row support with $\mathbf{R}_s(\boldsymbol{\Gamma}\mathbf{A})^H$ thereby $\mathbf{R}_s$. To fast reconstruct $\hat{\mathbf{S}}_{\hat{\theta}}$, inspired by [11–14], a new continuous function of complex-valued matrix, along with its complex-valued gradient matrix based maximization process, will be presented in the following. To replace the discontinuous $\|\widetilde{\mathbf{s}}_{\hat{\theta}}\|_0$, firstly, a continuous function corresponding to $\hat{\theta}_l$, is proposed as follows

$$f_l = \beta_l \exp\left\{-\sum_{n=1}^{N}[Re^2\{\hat{\mathbf{S}}_{\hat{\theta}}(l,n)\} + Im^2\{\hat{\mathbf{S}}_{\hat{\theta}}(l,n)\}]/2\sigma^2\right\} \tag{17}$$

where $Re\{\cdot\}$ and $Im\{\cdot\}$ denote the parameters corresponding to the real part and the imaginary part of $\{\cdot\}$, respectively. The coefficient β_l is calculated by $\beta_l = \|[\boldsymbol{\Gamma}\mathbf{a}(\hat{\theta}_l)]^H\mathbf{U}_n\|_2/\max\{\{\|[\boldsymbol{\Gamma}\mathbf{a}(\hat{\theta}_l)]^H\mathbf{U}_n\|_2\}_{l=1}^{L}\}$, and the noise subspace $\mathbf{U}_n$ consists of the eigenvectors corresponding to the smallest $N-P$ eigenvalues of $\mathbf{R}_x$. $\hat{\mathbf{S}}_{\hat{\theta}}(l,n)$ is the (l,n)th element of $\hat{\mathbf{S}}_{\hat{\theta}}$. The parameter σ is a number small enough for the desired accuracy.

In the viewpoint of the SR-based DOA estimation, the lth row of $\hat{\mathbf{S}}_{\hat{\theta}}$ satisfies $\|(\hat{\mathbf{S}}_{\hat{\theta}})_{(l,:)}\|_2 = \widetilde{\mathbf{s}}_{\hat{\theta}}(l) \gg \sigma$ if $\hat{\theta}_l$ corresponds to one of the true target DOAs. This results in $e^{-\sum_{n=1}^{N}[Re^2\{\hat{\mathbf{S}}_{\hat{\theta}}(l,n)\}+Im^2\{\hat{\mathbf{S}}_{\hat{\theta}}(l,n)\}]/2\sigma^2} \to 0$ based on the principles of the function limit, and simultaneously, $\beta_l \to 0$ because of the orthogonality between the signal and noise subspaces. Hence, in this case, we can conclude that $f_l \approx 0$ according to the designed construction of f_l in Eq. (17). On the other hand, if $\hat{\theta}_l$ is the direction sample outside the true target DOAs, $\|(\hat{\mathbf{S}}_{\hat{\theta}})_{(l,:)}\|_2 = \widetilde{\mathbf{s}}_{\hat{\theta}}(l) \ll \sigma$ and $\beta_l \to 1$ lead to $f_l \approx 1$. As the l_0-norm of $\widetilde{\mathbf{s}}_{\hat{\theta}}$ is the total number of non-zero entries in the sparse vector $\widetilde{\mathbf{s}}_{\hat{\theta}}$, the relationship between $\|\widetilde{\mathbf{s}}_{\hat{\theta}}\|_0$ and f_l is

$$\|\widetilde{\mathbf{s}}_{\hat{\theta}}\|_0 \approx L - \sum_{l=1}^{L} f_l = L - \widetilde{f} \tag{18}$$

where $\widetilde{f} = \sum_{l=1}^{L} f_l$. By this way, the discontinuous $\|\widetilde{\mathbf{s}}_{\hat{\theta}}\|_0$ is replaced by $L-\widetilde{f}$. Therefore, the signal reconstruction for the smoothed sparse DOA estimation can be reformulated as

$$\hat{\mathbf{S}}_{\hat{\theta}} = \arg\max(\widetilde{f}), \quad \text{s.t.} \quad \widetilde{\mathbf{R}}_{\widetilde{x}} = \boldsymbol{\Gamma}\hat{\mathbf{A}}_{\hat{\theta}}\hat{\mathbf{S}}_{\hat{\theta}} \tag{19}$$

The thorough and complete theoretical analysis provided in [13] has justified that the application of the smoothed l_0-norm sparse signal reconstruction technique can provide outstanding performance in a desired speed. Therefore, the gradient based signal recovery scheme [13] will be further applied in the following to fast solve the smoothed l_0-norm minimization, i.e. the $\widetilde{f}$ maximization problem in Eq. (19). Firstly, we derive a gradient matrix $\nabla_{\hat{\mathbf{S}}_{\hat{\theta}}}\widetilde{f}$ for the complex-valued matrix $\hat{\mathbf{S}}_{\hat{\theta}}$, which is required for the maximization based signal recovery. A gradient of $\widetilde{f}$ regarding the complex $\hat{\mathbf{S}}_{\hat{\theta}}(l,n)$ is defined as the following

$$\nabla_{\hat{\mathbf{S}}_{\hat{\theta}}(l,n)}\widetilde{f} = \frac{\partial\widetilde{f}}{\partial Re\{\hat{\mathbf{S}}_{\hat{\theta}}(l,n)\}} + j\frac{\partial\widetilde{f}}{\partial Im\{\hat{\mathbf{S}}_{\hat{\theta}}(l,n)\}} \tag{20}$$

where $\frac{\partial\widetilde{f}}{\partial k}$ stands for the partial derivative of $\widetilde{f}$ with respect to the parameter k. According to the definition of $\widetilde{f}$ in Eqs. (17) and (18), we can derive that

$$\frac{\partial\widetilde{f}}{\partial Re\{\hat{\mathbf{S}}_{\hat{\theta}}(l,n)\}} = \beta_l e^{-\sum_{n=1}^{N}\frac{|\hat{\mathbf{S}}_{\hat{\theta}}(l,n)|^2}{2\sigma^2}}\frac{\partial\left[-\sum_{n=1}^{N}\frac{|\hat{\mathbf{S}}_{\hat{\theta}}(l,n)|^2}{2\sigma^2}\right]}{\partial Re\{\hat{\mathbf{S}}_{\hat{\theta}}(l,n)\}} \tag{21}$$

with

$$\frac{\partial[-\sum_{n=1}^{N}|\hat{\mathbf{S}}_{\hat{\theta}}(l,n)|^2/2\sigma^2]}{\partial Re\{\hat{\mathbf{S}}_{\hat{\theta}}(l,n)\}} = -\frac{Re\{\hat{\mathbf{S}}_{\hat{\theta}}(l,n)\}}{\sigma^2} \tag{22}$$

where $|\cdot|$ denotes the modulus. As a result, we have

$$\frac{\partial\widetilde{f}}{\partial Re\{\hat{\mathbf{S}}_{\hat{\theta}}(l,n)\}} = -\frac{\beta_l Re\{\hat{\mathbf{S}}_{\hat{\theta}}(l,n)\}}{\sigma^2}e^{-\sum_{n=1}^{N}\frac{|\hat{\mathbf{S}}_{\hat{\theta}}(l,n)|^2}{2\sigma^2}} \tag{23}$$

Similar to Eq. (21)–(23), it can be found that

$$\frac{\partial\widetilde{f}}{\partial Im\{\hat{\mathbf{S}}_{\hat{\theta}}(l,n)\}} = -\frac{\beta_l Im\{\hat{\mathbf{S}}_{\hat{\theta}}(l,n)\}}{\sigma^2}e^{-\sum_{n=1}^{N}\frac{|\hat{\mathbf{S}}_{\hat{\theta}}(l,n)|^2}{2\sigma^2}} \tag{24}$$

Then the final result of the complex-valued gradient is

$$\nabla_{\hat{\mathbf{S}}_{\hat{\theta}}(l,n)}\widetilde{f} = -\frac{\beta_l\hat{\mathbf{S}}_{\hat{\theta}}(l,n)}{\sigma^2}e^{-\sum_{n=1}^{N}|\hat{\mathbf{S}}_{\hat{\theta}}(l,n)|^2/2\sigma^2} \tag{25}$$

Based on $\nabla_{\hat{\mathbf{S}}_{\hat{\theta}}(l,n)}\widetilde{f}$, a gradient matrix of $\widetilde{f}$ regarding the complex matrix $\hat{\mathbf{S}}_{\hat{\theta}}$ is constructed as

$$\nabla_{\hat{\mathbf{S}}_{\hat{\theta}}}\widetilde{f} = \begin{bmatrix}\nabla_{\hat{\mathbf{S}}_{\hat{\theta}}(1,1)}\widetilde{f},\ldots,\nabla_{\hat{\mathbf{S}}_{\hat{\theta}}(1,N)}\widetilde{f}\\ \vdots \\ \nabla_{\hat{\mathbf{S}}_{\hat{\theta}}(L,1)}\widetilde{f},\ldots,\nabla_{\hat{\mathbf{S}}_{\hat{\theta}}(L,N)}\widetilde{f}\end{bmatrix} \tag{26}$$

With $\nabla_{\hat{\mathbf{S}}_{\hat{\theta}}}\widetilde{f}$, the proposed method performs the maximization process in Eq. (19) as follows. An initial matrix is calculated from $(\hat{\mathbf{S}}_{\hat{\theta}})_0 = (\boldsymbol{\Gamma}\hat{\mathbf{A}}_{\hat{\theta}})^+\widetilde{\mathbf{R}}_{\widetilde{x}}$, and $(\cdot)^+$ is the pseudo-inverse operator. The parameter σ is set as a decreasing sequence $[\sigma_1,\sigma_2,\ldots,\sigma_K]$. Note that the approximation between $\|\widetilde{\mathbf{s}}_{\hat{\theta}}\|_0$ and $L-\widetilde{f}$ requires a small σ. However, a larger σ results in the improvement of the computational speed. For each σ_k,Z iterations are performed. In each iteration, $\hat{\mathbf{S}}_{\hat{\theta}}$ is updated as $\hat{\mathbf{S}}_{\hat{\theta}} \leftarrow \hat{\mathbf{S}}_{\hat{\theta}} - \mu(-\sigma^2\nabla_{\hat{\mathbf{S}}_{\hat{\theta}}}\widetilde{f})$ with $\mu \geqslant 1$. Then it is projected back to the feasible set, i.e.

$$\hat{\mathbf{S}}_{\hat{\theta}} \leftarrow \hat{\mathbf{S}}_{\hat{\theta}} - \left(\boldsymbol{\Gamma}\hat{\mathbf{A}}_{\hat{\theta}}\right)^+[(\boldsymbol{\Gamma}\hat{\mathbf{A}}_{\hat{\theta}})\hat{\mathbf{S}}_{\hat{\theta}} - \widetilde{\mathbf{R}}_{\widetilde{x}}] \tag{27}$$

The final reconstructed result is the output complex matrix of the Zth iteration for $\sigma = \sigma_K$. Thus the target DOA locations in the sample grid are obtained by searching the first P peaks, i.e.

$$\{\hat{l}_p\}_{p=1}^{P} = \arg\max_{l}\{\|\left(\hat{\mathbf{S}}_{\hat{\theta}}\right)_{(l,:)}\|_2,\ l \in [1,\ldots,L]\} \tag{28}$$

The covariance matrix based fast sparse DOA estimation for partly calibrated array is then completed, i.e. $\{\hat{\theta}_{\hat{l}_1},\hat{\theta}_{\hat{l}_2},\ldots,\hat{\theta}_{\hat{l}_P}\}$.

4. Simulation results

Some representative simulations are carried out to verify the estimation performance and computational speed of the proposed method. The signals and noises described in Eq. (1) are considered. The direction sample grid is from −90° to 90°, with 0.1° interval for all analyzed DOA estimation methods. The parameters in the proposed method are preset as $\sigma_1 = 14\max\{|(\hat{\mathbf{S}}_{\hat{\theta}})_0|\}, \sigma_{k+1} = 0.5\sigma_k \geqslant 0.0005, \mu = 2.5$ and $Z = 4$. The regularization precision parameters for the l_1-SVD method [6] with the proposed error matrix estimation, the adaptive SR method [20] and the joint optimization method [21] are the asymptotic chi-square distribution upon normalization by the variance of the noises, with NP, N and NT degrees of freedom, respectively. All results are obtained from 400 Monte Carlo trials.

A 9-sensor partly calibrated ULA impinged by the signals from three uncorrelated targets is considered. For all of the simulations except for Fig. 4 that evaluates the effects of different error degrees on the

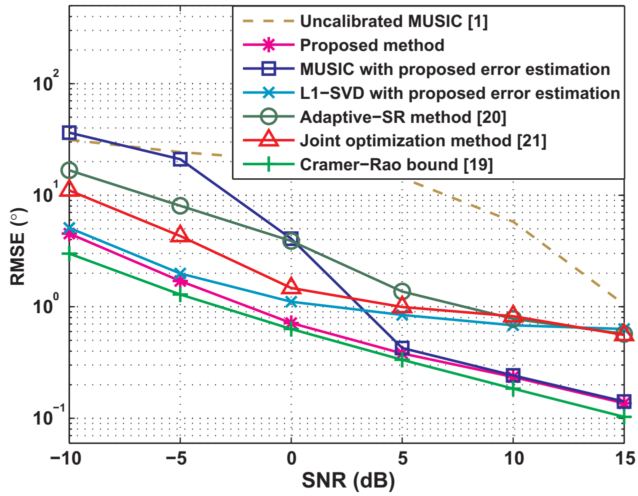

Fig. 1. RMSE versus SNR.

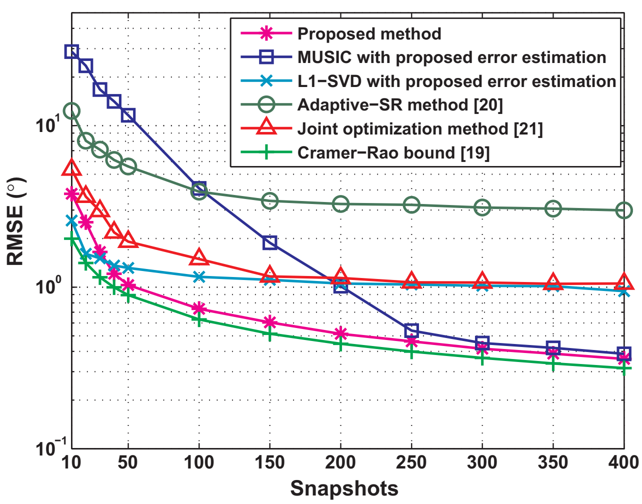

Fig. 2. RMSE versus snapshots.

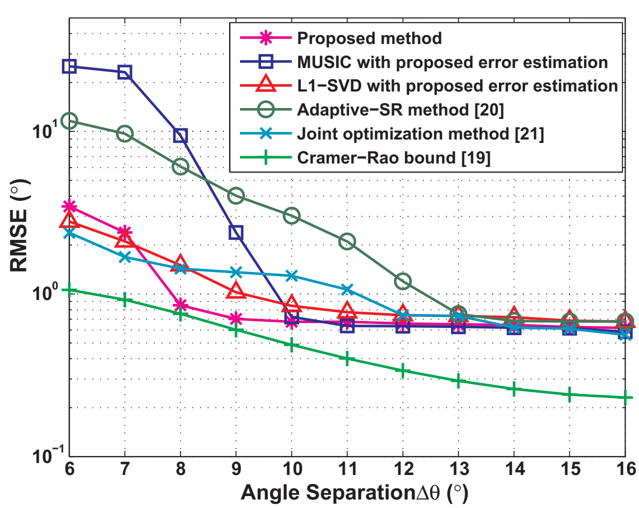

Fig. 3. RMSE versus angle separation.

performance of DOA estimation, the gain-phase errors are fixedly set as $\left[0.75e^{\frac{j\pi}{14}},0.7e^{-\frac{j\pi}{75}},0.8e^{\frac{j\pi}{54}},0.9e^{\frac{j\pi}{23}},1.15e^{-\frac{j\pi}{20}}\right]$ with $m = 4$. In addition, the DOAs $\theta_1 = -8.2°,\theta_2 = 0°$ and $\theta_3 = 9.3°$ are considered in all the simulations except Fig. 3, whose target DOAs are $\theta_1 = -\Delta\theta,\theta_2 = 0°$ and

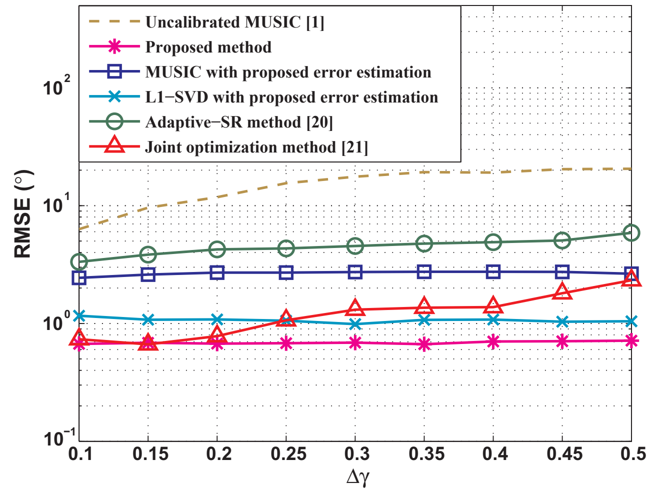

(a) RMSE versus different degrees of gain errors.

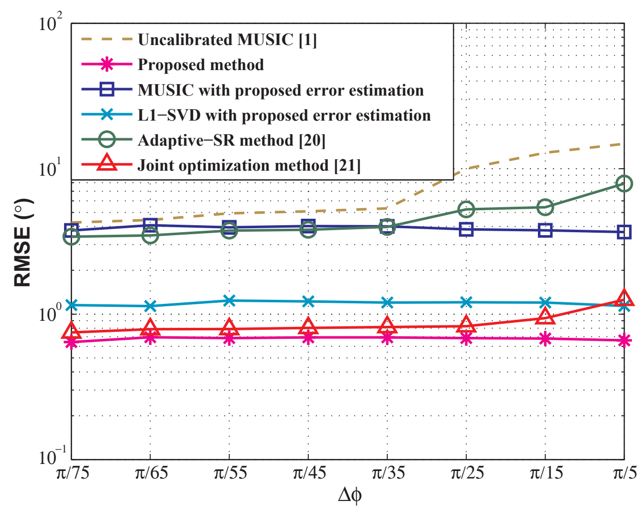

(b) RMSE versus different degrees of phase errors.

Fig. 4. RMSE versus different degrees of gain-phase errors.

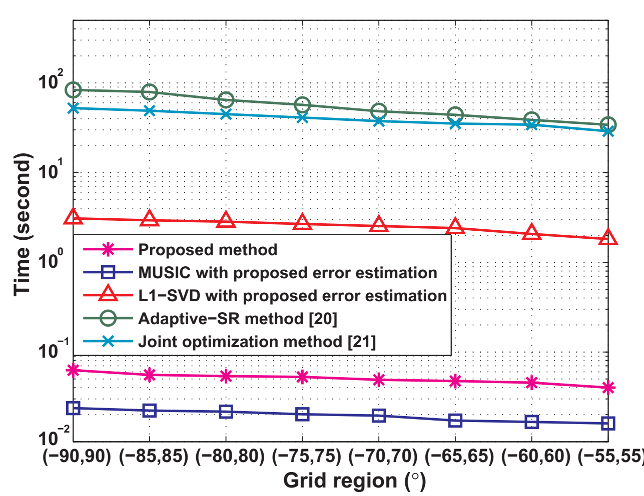

Fig. 5. Computation time versus grid region.

$\theta_3 = \Delta\theta$ with variational $\Delta\theta$ to demonstrate the influence of different angle separations.

Fig. 1 shows the root mean square error (RMSE) of DOA estimation versus SNR, where $T = 100$. It verifies that for a wide range of SNR, the

Table 1
Computation time of different methods (second).

T	20	50	80	100
Proposed method	0.0615	0.0622	0.0624	0.0627
l_1-SVD	2.8781	2.9034	2.9446	3.0856
Adaptive SR	16.8846	41.5287	66.2565	82.9858
Joint optimization	12.3651	27.6852	38.0406	52.4046
MUSIC	0.0218	0.0229	0.0233	0.0237

proposed new method provides the best performance among all the algorithms in consideration. In addition, when applied to other methods, the proposed error estimation is effective for partly calibrated ULA. The l_1-SVD algorithm [6] with the proposed error matrix estimation can achieve better DOA estimation than the adaptive SR [20] and the joint optimization [21] methods. However, the subspace based MUSIC with the proposed error matrix estimation performs worse than the sparse DOA estimation methods at low SNR region for SNR $<$ 0 dB.

Fig. 2 shows the relationship between RMSE and the number of snapshots with SNR = 0 dB. From Fig. 2, it can be seen that the proposed method is superior to the other methods when $T > 40$. Besides, the performance of the MUSIC with the proposed error matrix estimation is inferior to that of the others for small snapshots.

Fig. 3 shows RMSE versus angle separation $\Delta\theta$, where SNR = 0 dB and $T = 100$. It verifies that the RMSE of the proposed method decreases with the increase of $\Delta\theta$, and reaches an asymptotic value at about $\Delta\theta = 10°$. For closely located targets, the performance of the proposed method is close to that of the l_1-SVD algorithm with the proposed error matrix estimation. However, the MUSIC based method provides the worst DOA estimation performance for small angle separation.

Fig. 4(a) and (b) demonstrates the impacts of the degrees of gain errors and phase errors on the DOA estimation performance, respectively. In Fig. 4, SNR = 0 dB, and the other simulation conditions keep the same with those of Fig. 1. Moreover, the error matrix is generated by $\{\boldsymbol{\Gamma}_{(n,n)}\}_{n=1}^{4} = 1, \{\boldsymbol{\Gamma}_{(n,n)}\}_{n=5}^{7} = (1-\Delta\gamma)e^{-j\Delta\varphi}$ and $\{\boldsymbol{\Gamma}_{(n,n)}\}_{n=8}^{9} = (1+\Delta\gamma)e^{j\Delta\varphi}$. For Fig. 4(a) with variable $\Delta\gamma$ and Fig. 4(b) with variable $\Delta\varphi$,$\Delta\varphi$ and $\Delta\gamma$ are respectively set as zeros. As can be seen from Fig. 4, the performance of the proposed method is not affected by the variations of the gain and the phase errors. However, both of the gain errors and the phase errors can cause the degradations on the DOA estimation performance of the methods in [20,21], as verified in Fig. 4(a) and (b).

Corresponding to Fig. 4, the computation time is shown in Fig. 5. Different grid regions with different numbers of grid cells are considered. The computational complexity of the MUSIC with the proposed error matrix estimation is about $O[N^2T + N(N-P)L]$. Besides, the proposed method, the l_1-SVD method [6] with the proposed error matrix estimation, the adaptive SR method [20] with $\widetilde{Z}_1$ iterations and the joint optimization method [21] with $\widetilde{Z}_2$ iterations, need about $O[N^2T + N^2LZK]$,$O[N^2T + (LP)^3]$,$O[L^3T\widetilde{Z}_1]$ and $O[(L^2N + L^2T)\widetilde{Z}_2]$ computation burden, respectively. Note that as recommended in their own schemes, the method in [21] uses the alternating direction method of multipliers (ADMM) [23] to solve its two convex optimization subproblems, and the methods in [6,20] use the SOC (second order cone) programming software package SeDuMi [24] for their convex optimization. When L decreases, the speed is improved. Although the MUSIC based method has lower complexity than the proposed method, it performs worse for low SNR region, snapshot deficiency and small angle separation. The proposed method requires the least amount of time in all of the analyzed sparse DOA estimation methods, as can be seen from Fig. 5.

For some snapshot cases at SNR = 0 dB, the computation time is compared in Table 1. It verifies that the proposed method is at least two orders of magnitude faster than the existing sparse DOA estimation methods for partly calibrated array.

5. Conclusion

In this paper, for partly calibrated array, we have proposed a fast smoothed sparse DOA estimation algorithm with a gain-phase error matrix estimation strategy. Firstly, we present the new error matrix estimation scheme without estimating each gain error separately. Then the signal reconstruction tailored for complex-valued covariance matrix is provided. The proposed method has much lower complexity than the other sparse DOA estimation methods with partly calibrated array. Simulation results demonstrate that it performs well and is independent of the errors.

Acknowledgment

This work was supported by the China Scholarship Council (CSC, No. 201506680027), and the Fundamental Research Funds for the Central Universities (HEUCF160401).

References

[1] Stoica P, Nehorai A. MUSIC, maximum likelihood, and Cramer-Rao bound. IEEE Trans Signal Process 1989;37(5):720–41.
[2] Cui KB, Wu WW, Huang JJ, Chen X, Yuan NC. DOA estimation of LFM signals based on STFT and multiple invariance ESPRIT. Int J Electron Commun (AEU) 2017;77:10–7.
[3] Viberg M, Ottersten B. Sensor array processing based on subspace fitting. IEEE Trans Signal Process 1991;39(5):1110–21.
[4] Yan FG, Shen Y, Jin M. Fast DOA estimation based on a split subspace decomposition on the array covariance matrix. Signal Process 2015;115:1–8.
[5] Liu YY, Sun XY, Zhao SS. A covariance matrix shrinkage method with Toeplitz rectified target for DOA estimation under the uniform linear array. Int J Electron Commun (AEU) 2017;81:50–5.
[6] Malioutov D, Cetin M, Willsky AS. A sparse signal reconstruction perspective for source localization with sensor arrays. IEEE Trans Signal Process 2005;53(8):3010–22.
[7] Wang XP, Wang W, Liu J, Li X, Wang JX. A sparse representation scheme for angle estimation in monostatic MIMO radar. Signal Process 2014;104(11):258–63.
[8] Liu J, Zhou WD, Wang XP. Fourth-order cumulants-based sparse representation approach for DOA estimation in MIMO radar with unknown mutual coupling. Signal Process 2016;128(11):123–30.
[9] Zhang Y, Ye ZF, Xu X, Hu N. Off-grid DOA estimation using array covariance matrix and block-sparse Bayesian learning. Signal Process 2014;98(5):197–201.
[10] Tian Y, Xu H. DOA, power and polarization angle estimation using sparse signal reconstruction with a COLD array. Int J Electron Commun (AEU) 2015;69(11):1606–12.
[11] Mohimani GH, Babaie-Zadeh M, Jutten C. Fast sparse representation based on smoothed l^0 norm. In: International conference on independent component analysis and signal separation. Berlin (Heidelberg): Springer; 2007. p. 389–96.
[12] Mohimani GH, Babaie-Zadeh M, Jutten C. Complex-valued sparse representation based on smoothed l^0 norm. In: IEEE international conference on acoustics, speech and signal processing; 2008. p. 3881–4.
[13] Mohimani G H, Babaie-Zadeh M, Jutten C. A fast approach for overcomplete sparse decomposition based on smoothed l^0 norm. IEEE Trans Signal Process 2009;57(1):289–301.
[14] Liu J, Zhou WD, Juwono F H, Huang DF. Reweighted smoothed l_0-norm based DOA estimation for MIMO radar. Signal Process 2017;137:44–51.
[15] Liu J, Zhou WD, Juwono F H. Joint smoothed l_0-norm DOA estimation algorithm for multiple measurement vectors in MIMO radar. Sensors 2017;17(5):1068.
[16] Cao SH, Ye ZF, Xu DY, Xu X. A Hadamard product based method for DOA estimation and gain-phase error calibration. IEEE Trans Aerosp Electron Syst 2013;49(2):1224–33.
[17] Cao SH, Ye ZF, Hu N, Xu X. DOA estimation based on fourth-order cumulants in the presence of sensor gain-phase errors. Signal Process 2013;93:2581–5.
[18] Liu AF, Liao GS, Zeng C, Yang ZW, Xu Q. An eigenstructure method for estimating DOA and sensor gain-phase errors. IEEE Trans Signal Process 2011;59(12):5944–56.
[19] Liao B, Chan SC. Direction finding with partly calibrated uniform linear arrays. IEEE Trans Antennas Propag 2012;60(2):922–9.
[20] Sun K, Liu YM, Meng HD, Wang XQ. Adaptive sparse representation for source localization with gain/phase errors. Sensors 2011;11(5):4780–93.
[21] Liu HQ, Zhao LM, Li Y, Jing XR, Truong TK. A sparse-based approach for DOA estimation and array calibration in uniform linear array. IEEE Sens J 2016;16(15):6018–27.
[22] Yan H, Li J, Liao G. Multitarget identification and localization using bistatic MIMO radar systems. EURASIP J Adv Signal Process 2008;DOI:10.
[23] Boyd S, Parikh N, Chu E, Peleato B, Eckstein J. Distributed optimization and statistical learning via the alternating direction method of multipliers. Found Trends® Mach Learn 2011;3(1):1–122.
[24] Sturm JF. Using SeDuMi 1.02, a MATLAB toolbox for optimization over symmetric cones. Optim Method Softw 2009;11–12:625–53.